Soft Matter

Quantitative relationship between cholesterol distribution and ordering of lipids in asymmetric lipid bilayers

Journal:	*Soft Matter*
Manuscript ID	SM-ART-09-2020-001709.R2
Article Type:	Paper
Date Submitted by the Author:	21-Jan-2021
Complete List of Authors:	Aghaaminiha, Mohammadreza; Ohio University, Chemical and Biomolecular Engineering Farnoud, Amir; Ohio University, Chemical and Biomolecular Engineering Sharma, Sumit; Ohio University, Chemical and Biomolecular Engineering

Quantitative relationship between cholesterol distribution and ordering of lipids in asymmetric lipid bilayers

Mohammadreza Aghaaminiha[a], Amir M. Farnoud[a], Sumit Sharma[a,*]

[a]Department of Chemical and Biomolecular Engineering, Russ College of Engineering and Technology, Ohio University, Athens, OH 45701, USA

***Corresponding author: Email:** sharmas@ohio.edu

Keywords: Cholesterol, membrane asymmetry, lipid bilayer, molecular dynamics

Abstract

The plasma membrane of eukaryotic cells is known to be compositionally asymmetric. Certain phospholipids, such as sphingomyelin and phosphatidylcholine species, are predominantly localized in the outer leaflet, while phosphatidylethanolamine and phosphatidylserine species primarily reside in the inner leaflet. While phospholipid asymmetry between the membrane leaflets is well established, there is no consensus about cholesterol distribution between the two leaflets. We have performed a systematic study, via molecular simulations, of how the spatial distribution of cholesterol molecules in different "asymmetric" lipid bilayers are affected by the lipids' backbone, head-type, unsaturation, and chain-length by considering an asymmetric bilayer mimicking the plasma membrane lipids of red blood cells, as well as seventeen other asymmetric bilayers comprising of different lipid types. Our results reveal that the distribution of cholesterol in the leaflets is solely a function of the extent of ordering of the lipids within the leaflets. The ratio of the distribution of cholesterol matches the ratio of lipid order in the two leaflets, thus providing a quantitative relationship between the two. These results are understood by the observation that asymmetric bilayers with equimolar amount of lipids in the two leaflets develop tensile and compressive stresses due to differences in the extent of lipid order. These stresses are alleviated by the transfer of cholesterol from the leaflet in compressive stress to the one in tensile stress. These findings are important in understanding the biology of the cell membrane, especially with regard to the composition of the membrane leaflets.

1. Introduction

The plasma membrane is a lipid bilayer that separates the cell from the outside environment.[1–3] While different mammalian cells are known to have a wide variety of lipids in their plasma membrane, it is now well-understood that the phospholipid composition of the inner (cytofacial) leaflet in all mammalian cells is different from that of the outer (exofacial) leaflet.[4–6] Verkleij et al. pioneered studies on phospholipid asymmetry, showing that sphingomyelin (SM) and phosphatidylcholine (PC) are abundant in the outer leaflet, while phosphatidylethanolamine (PE) and phosphatidylserine (PS) are primarily localized in the inner leaflet.[7] These findings were later verified by the recent studies of Lorent et al.[5] and Vahedi et al.[8] The phospholipid asymmetry in membrane leaflets has important functional implications for the cell. For instance, in healthy red blood cells, PS is known to be almost exclusively localized in the inner leaflet, the presence of this lipid in the outer leaflet is a sign of eryptosis and a signal to macrophages to phagocytose the old red blood cells and maintain homeostasis.[4,9]

While the asymmetry of phospholipids in the plasma membrane is well-established, there is little consensus regarding cholesterol distribution in different leaflets of the plasma membrane.[4,6,10] Unlike phospholipids, there are no specific enzymes for cholesterol transport across the bilayer, and cholesterol distribution is believed to be primarily dictated by its affinity towards other lipids.[4,10] However, experimental results in this regard have been contradictory. It has been reported that cholesterol molecules are enriched in the outer leaflet because of their strong interactions with the saturated acyl chain phospholipids, specifically SM.[11–14] Contrarily, it has also been suggested that the inner leaflet is favored by cholesterol due to (i) the abundance of PE phospholipids in this leaflet which provides higher negative curvature,[15,16] and (ii) the abundance of C24 sphingolipids in the outer leaflet which pushes cholesterol to the inner leaflet.[17] There are also other reports that mention that cholesterol is symmetrically distributed in the cell membrane.[18,19]

Experimental studies of cholesterol distribution are complicated by several confounding factors. First, different mammalian cells have different membrane lipid compositions.[20,21] Secondly, experimental methods such as quenching of dehydroergosterol fluorescence, filipin staining, noninvasive neutron scattering, and enzymatic degradation by cholesterol oxidase, while helpful, each suffer from various drawbacks.[22,23] Finally, cholesterol is known to flip-flop between the two leaflets at a rapid rate, [24–27] making it difficult for experimental probes to trace it with high accuracy at any time-point.[28] A mechanistic study on how changes in lipid structure and chemistry affect cholesterol distribution helps to provide a general understanding of cholesterol asymmetry in the plasma membrane.

In the current work, we have studied the spatial distribution of cholesterol within asymmetric lipid bilayers via coarse-grained (CG) molecular dynamics (MD) simulations. We have performed two sets of simulations, with the first focusing on characterizing cholesterol distribution in a lipid bilayer mimicking the known membrane lipid composition of red blood cells and the second focusing on elucidating how the structure and chemistry of the lipids in the bilayer affect cholesterol distribution. Results reveal that the ordering of lipids in membrane leaflets is the primary regulator of cholesterol spatial distribution in the asymmetric bilayers.

2. Methodology

2.1. Force Field

We have employed the coarse-grained (CG) Wet Martini force field with polarizable water to model all lipids, cholesterol, ions, and water molecules in the system. The polarizable water model for the Martini force field, developed by Yesylevskyy et al.,[30,31] is a three-bead model to represent four water molecules and can capture the orientational polarizability and the dielectric screening effect of bulk water. The topologies of lipids are described in **Figures S1** and **S2** alongside the name and type of each bead. The main types of particles in the Martini CG force field are P, polar; N, intermediate; C, apolar; and Q, charged. Subscripts *0*, *a*, *d*, and *da* indicate if the particle has hydrogen-bond (H-bond) forming capacities. The particle with "*0*" has no H-bond capacity, "*a*" is a H-bond acceptor, "*d*" is a H-bond donor, and "*da*" is both H-bond acceptor and donor.[32] Other subscripts are numbers: 1, 2, 3, 4, and 5 that display the degree of polarity, where 5 is the most and 1 is the least polar particle.[32]

2.2. Simulation Details

Periodic boundary conditions were applied in all three directions of the simulation box. In the first set of simulations (**Figure S1**), the simulation box size was 250 × 250 × 125 (Å^3), the total number of lipids in the systems was 2,043, and the total number of water molecules was 41,487. In the second set of simulations (**Figure S2**), the simulation box size was 125 Å in all directions, the total number of lipids in the systems was 510, and the total number of water molecules was 10,834. Initial configuration of lipid bilayers was generated using the *Insane.py* script developed by Marrink et al.[33] All simulations were performed on the GROMACS/5.1.2 molecular simulation package.[34]

The initial configuration of the system was energy minimized by employing steepest descent algorithm with the maximum force tolerance of 1000.0 kJ.mol^{-1}.nm^{-1}. This was followed by a 25 ns canonical ensemble (constant number of particles N, volume V, and temperature T) simulation and a 25 ns isothermal-isobaric (constant N, pressure P, T) ensemble simulation for pre-equilibration. The time-step chosen for

both the ensembles was 10 fs. Then, three replicas of 10 μs NPT simulation with a timestep of 20 fs were performed, as in previous studies [3], and the data was collected for the last 6 μs for all the simulations.

The parameters of the simulation system parameters were chosen to be the same as in the previous work done to parameterize the polarizable water model on the Martini force field.[31] Briefly, a spherical cut-off of 1.1 nm was chosen for the Lennard Jones (LJ) interactions. For Coulombic interactions, Reaction-Field-zero (RF-zero) was employed with the spherical cut-off of 1.1 nm.[31] The RF-zero and PME (Particle Mesh Ewald) electrostatics have been systematically compared previously and no differences in the bilayer properties were identified.[31] The relative dielectric constant was taken to be 2.5.[30,31] Both LJ and Coulombic interactions were smoothly shifted to be zero beyond the cut-off. In the short pre-equilibration runs, Berendsen thermostat and barostat with the time constants of 1 ps and 3 ps, respectively were employed for quick equilibration. For the NPT equilibration and production runs, the velocity-rescaling thermostat developed by Bussi et al.[35] was used. Semi-isotropic pressure coupling was accomplished using Parrinello-Rahman barostat with the coupling time constant of 12 ps.[3,31] Along the axis of the bilayer plane and the z-direction, the reference pressure and isothermal compressibility were set to be 1.0 bar and 3×10^{-4} bar^{-1}, respectively. All simulations are performed at 37 ^{o}C.

Radial distribution functions, g(r), were calculated to examine the proximity of the hydroxyl headgroup of cholesterol (ROH CG bead) to various chemical moieties in phospholipids. Pioneering work by Huang has described the importance of the proximity of the –OH group of sterols, in the β configuration, to the carbonyl oxygen of the fatty acyl groups in phospholipids for strong cholesterol-lipid interactions.[36]

We divide the bilayer into three regions, namely, inner leaflet, midplane, and outer leaflet. The threshold for separating these regions was set to be 0.8 nm from the center of the bilayer as previously suggested.[2,3] Cholesterol flip-flop rate was defined as the average frequency by which the cholesterol molecules undergo intramembrane exchange, in other words, leave the inner/outer leaflet, reach the outer/inner leaflet, and then return to the inner/outer leaflet.[24,25,37] Orientation of a cholesterol molecule within a bilayer was defined as the angle between vector, $\bar{a}$ (the vector joining the ROH bead to the C1 bead of cholesterol, see **Figure S1**) and vector $\bar{z}$ (the bilayer normal). To measure the ordering of lipids in each leaflet, ensemble-averaged order parameter of the acyl chains of lipids[38,39] was calculated , as in **Equation 1**:

$$S_{Chain} = \left\langle \frac{1}{2}\left(3\langle cos^2\theta\rangle - 1\right)\right\rangle \qquad \text{Equation 1}$$

Where θ is the angle between each bond vector of the acyl chain beads and the bilayer normal. A high value of the S_{Chain} (~ 1) indicates that the bonds are aligned with the bilayer normal, whereas a low value (~ 0) indicates that the bonds are randomly oriented respect to the bilayer normal.[38,39] The area per lipid,

a(x) for each leaflet was calculated based on the ensemble-averaged area of the plane in the simulation box, *A(x)* divided by the total number of two-chain lipids + cholesterols in that leaflet (*x* is the mole fraction of cholesterol in the system).[40]

$$a(x) = \frac{A(x)}{N_{lipids} + N_{chol}} \qquad \text{Equation 2}$$

The thickness of the bilayer was estimated as the ensemble-averaged distance between the phosphate head group of the lipids (PO4 CG bead shown in **Figure S1**) in the two leaflets.[40,41]

3. Results and Discussion

3.1. Cholesterol distribution in the leaflets of the bilayer

The asymmetric distribution of lipids in the plasma membrane is expected to affect the localization of cholesterol in membrane leaflets. To examine this phenomenon, an asymmetric lipid bilayer, mimicking the lipid composition of the plasma membrane of red blood cells was studied. The asymmetric lipid bilayer comprised of seven different lipids. The outer leaflet lipids were selected to be POPC/16:0SM/POPE/CHOL with the molar ratio of 31/29/7/33 while the inner leaflet lipids were DOPC/16:1SM/DOPE/DOPS/CHOL with the molar ratio of 10/7/31/19/33. This composition of phospholipids matches the predominant lipids in each leaflet of the plasma membrane of red blood cells.[5,7,8] Cholesterol was the only sterol included in the system with a molar ratio of 1:2 with respect to the total number of lipids in the two leaflets. Cholesterol content has been reported to be in the range of 30 mol% to 50 mol% in mammalian cell plasma membranes.[42,43] Two symmetric model lipid bilayers were also studied. In the first bilayer, labeled cyto-symmetric, the two leaflets had the same lipid composition as that of the inner (cytofacial) leaflet of the asymmetric bilayer noted above. In the second symmetric bilayer, labeled exo-symmetric, the composition of both leaflets was the same as the outer (exofacial) leaflet of the asymmetric bilayer. The lipid compositions of the three systems are listed in **Table 1**.

Table 1. Composition of the inner and outer leaflets of the lipid bilayers studied in this work. Cholesterol was included in all the bilayers with the molar ratio of 1:2 with respect to the total number of lipids.

System	Inner leaflet	Outer leaflet
Asymmetric	DOPC/16:1SM/DOPE/DOPS/CHOL: 10/7/31/19/33	POPC/16:0SM/POPE/CHOL: 31/29/7/33
Cyto-symmetric	DOPC/16:1SM/DOPE/DOPS/CHOL: 10/7/31/19/33	DOPC/16:1SM/DOPE/DOPS/CHOL: 10/7/31/19/33
Exo-symmetric	POPC/16:0SM/POPE/CHOL: 31/29/7/33	POPC/16:0SM/POPE/CHOL: 31/29/7/33

In the initial configuration, cholesterol molecules were equally distributed between the two leaflets. Upon equilibration of the simulation, cholesterol distribution became asymmetric in the bilayer with asymmetric lipid composition, and symmetric in case of the two symmetric bilayers, confirming the direct role of phospholipid chemistry in cholesterol localization (**Figure 1A**). In the asymmetric bilayer, the fraction of cholesterol molecules in the inner and outer leaflets were 41 ± 1% and 53 ± 2%, respectively, while 6 ± 2% of cholesterol resided in the midplane of the bilayer. In the cyto-symmetric bilayer, mimicking the inner leaflet, a larger fraction of cholesterol was found in the midplane (11 ± 3% compared to 6 ± 2% for the asymmetric bilayer), while the exo-symmetric bilayer only had 3 ± 1% of cholesterol molecules in the midplane. This result is consistent with the experiments showing that cholesterol have a preference for the bilayer midplane in the case of polyunsaturated bilayers.[44]

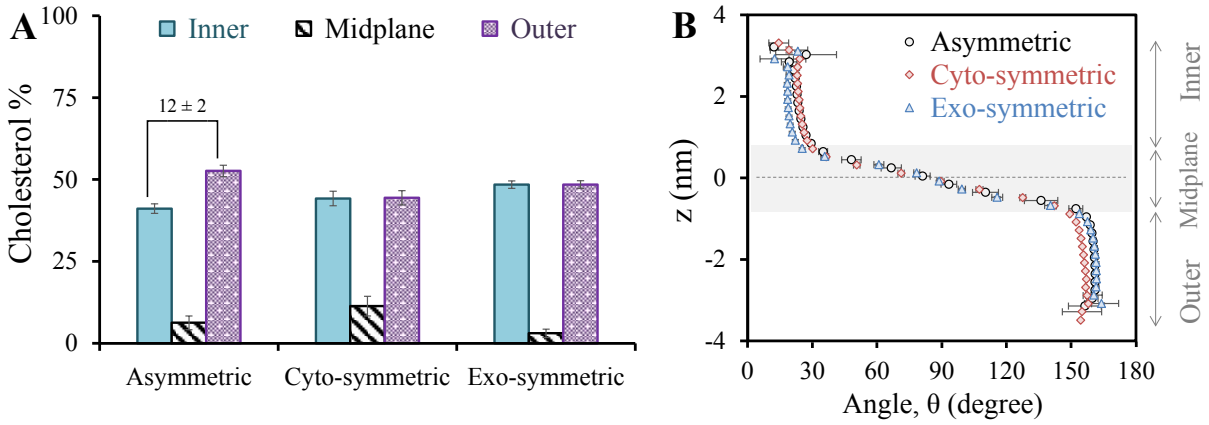

Figure 1. A) Percentage of cholesterol molecules located in the inner leaflet (cyan), midplane (black striped), and the outer leaflet (purple) of the asymmetric, cyto-symmetric, and exo-symmetric lipid bilayers. **B)** Ensemble-averaged angle of cholesterol molecule with the bilayer normal as a function of the location of the hydroxyl headgroup of cholesterol. Shaded area represents the midplane of the bilayer. Beyond the midplane, the orientation is almost independent of the location. Error bars in both the figures were estimated as standard error of the mean when the last 6 μs of the three replicas of each system were split into four equally sized blocks of 1.5 μs each.

Figure 1B shows the orientation of cholesterol molecules as a function of location within the bilayer for the three bilayers. For this calculation, the lipid bilayer was divided into ~30 slabs parallel to the plane of the bilayer. In each slab, the ensemble-averaged angle of the cholesterol molecules with respect to the bilayer normal was found. The reported angle with respect to the bilayer normal corresponds to the average over the configurations in the last 6 μs of three independent replicas of each system. Within 0.8 nm from the center of the bilayer, cholesterol orientation changes almost linearly with the distance from the center for all the three studied systems. At the distance of 0.8 nm from the center, a sharp change in the orientation of cholesterol is observed and so this region is defined as the midplane.[2]

It has been suggested that the alignment of cholesterol in the leaflet favors the cholesterol-lipid interaction in the PM.[36,45] Therefore, it is hypothesized that the ordering of lipids in a leaflet should favor the presence of cholesterol. Indeed, the outer leaflet of the asymmetric bilayer has a larger S_{Chain} (0.48±0.02) as compared to that of the inner leaflet (0.33±0.02). S_{Chain}, as defined in **Equation 1**, is a measure of ordering of the lipids in a leaflet; a high value of S_{Chain} corresponds to more order. The exo-symmetric and the cyto-symmetric bilayers have the S_{Chain} values of 0.48±0.02 and 0.32±0.02, respectively, for both leaflets, which explains the higher concentration of cholesterol in the exo-symmetric leaflets as compared to in the cyto-symmetric leaflets. These findings suggest that the ordering of the lipids in the leaflets is an important factor in determining the localization of cholesterol within the leaflets of the bilayer. Other physical characteristics of these bilayers, such as area per lipid and the thickness, were also compared and are listed in **Table S1** (Supporting Information). The cyto-symmetric is the thinnest and exo-symmetric is the thickest bilayer, as expected, but the difference in the thickness is only ~ 2 Å. The asymmetric bilayer has a slightly smaller area per lipid (0.52 ± 0.01 nm^2) at the inner leaflet as compared to the cyto-symmetric bilayer (0.52 ± 0.01 nm^2) and has slightly larger area per lipid (0.48 ± 0.01 nm^2) at the outer leaflet as compared to the exo-symmetric bilayer (0.47 ± 0.01 nm^2). This difference confirms that the asymmetry influences the properties of the leaflets.[46] The values of area per lipid are smaller than those usually reported for the bilayers where no cholesterol is present (~ 0.5 to 0.7 nm^2).[47]

It should be noted that the composition of lipids in different leaflets of the asymmetric bilayer did not get altered during the simulations. The density profiles of different lipids in the equilibrated bilayer confirm this point (**Figure S3**). On average, in the asymmetric bilayer only 2 out of 103 DOPC, 1 out of 74 SM, 7 out of 311 DOPE, and 6 out of 192 DOPS lipids moved from the inner leaflet to the outer leaflet, while no lipid molecule from the outer leaflet moved to the inner leaflet.

3.1. Cholesterol flip-flop rate

A large range of cholesterol flip-flop rates have been reported in previous simulations[24,25] and experiments.[23,48,49] It has been argued that chemical probes or markers that are employed for experimental measurements of the flip-flop rates influence the rates.[23] While some non-invasive but indirect measurements of the flip-flop rates[23] have been introduced, the predictions made from these methods have remained contentious.[22,29] Cholesterol flip-flop rate is understood to increase with temperature and the amount of unsaturated lipids[50] and decrease with the thickness of the bilayer.[9] However, there is little understanding of how the flip-flop rates are affected by changes in bilayer (a)symmetry. One would presume that the flip-flop rate in an asymmetric bilayer will be dictated by the rate determining step that is the slower flip-flop rate observed for the more ordered leaflet. Furthermore, previous investigations have not studied the distribution of cholesterol flip-flop rates. **Figure 2** shows the distribution of cholesterol flip-flop rates for the asymmetric, cyto-symmetric and exo-symmetric bilayers. The more ordered exo-symmetric bilayer showed the lowest average flip-flop rate of 0.77±0.03 μs^{-1}. The flip-flop rate of the asymmetric bilayer was found to be higher, 1.39±0.04 μs^{-1}. The flip-flop rate of the cyto-symmetric bilayer was the highest at 2.80±0.05 μs^{-1}. Interestingly, the distribution of flip-flop rates was symmetric around the mode value for cyto-symmetric bilayer, whereas for both the asymmetric and the exo-symmetric bilayer, the distribution was skewed. An interesting conclusion is drawn from this analysis that the cholesterol flip flop rates of asymmetric lipid bilayers is in-between the flip flop rates observed for symmetric bilayers made up of their individual leaflets.

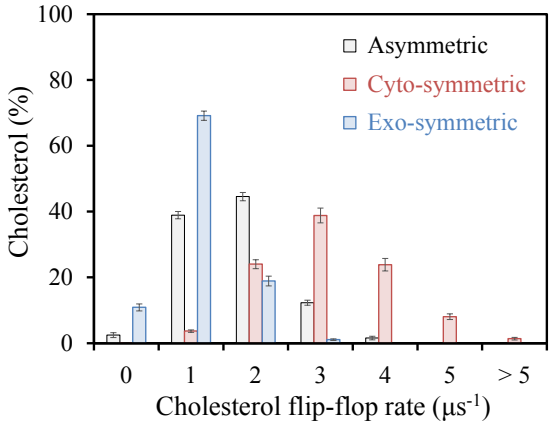

Figure 2. Distribution of cholesterol flip-flop rates for the three bilayers. Exo-symmetric bilayer with more ordered lipids has a narrower distribution with the smallest mode value. Cyto-symmetric bilayer has a broader distribution with the largest mode value. The flip-flop rate of the asymmetric bilayer is in-between the two symmetric bilayers. The error bars are estimated as the standard error of the mean when the last 6 μs of the simulations of three replicas of each system were split into four equally sized blocks.

3.2. Spatial arrangement of cholesterol molecules in the plane of the bilayer

Next, we analyzed the spatial arrangement of cholesterol and phospholipids within the leaflets of the asymmetric lipid bilayer via 2D radial distribution functions, $g_{2D}(r)$. **Figure 3A** and **B,** show that the ROH-AM and ROH-GL $g_{2D}(r)$ display a strong peak at the location of first coordination shell. First coordination shell can be thought of as the closest distance around a molecule that is accessible to other molecules. Therefore, this result suggests that there is a strong affinity of cholesterol molecules for the amide and glycerol beads of phospholipids (refer to **Figure S1C** for the representation of different CG Martini beads of the lipids and cholesterol).

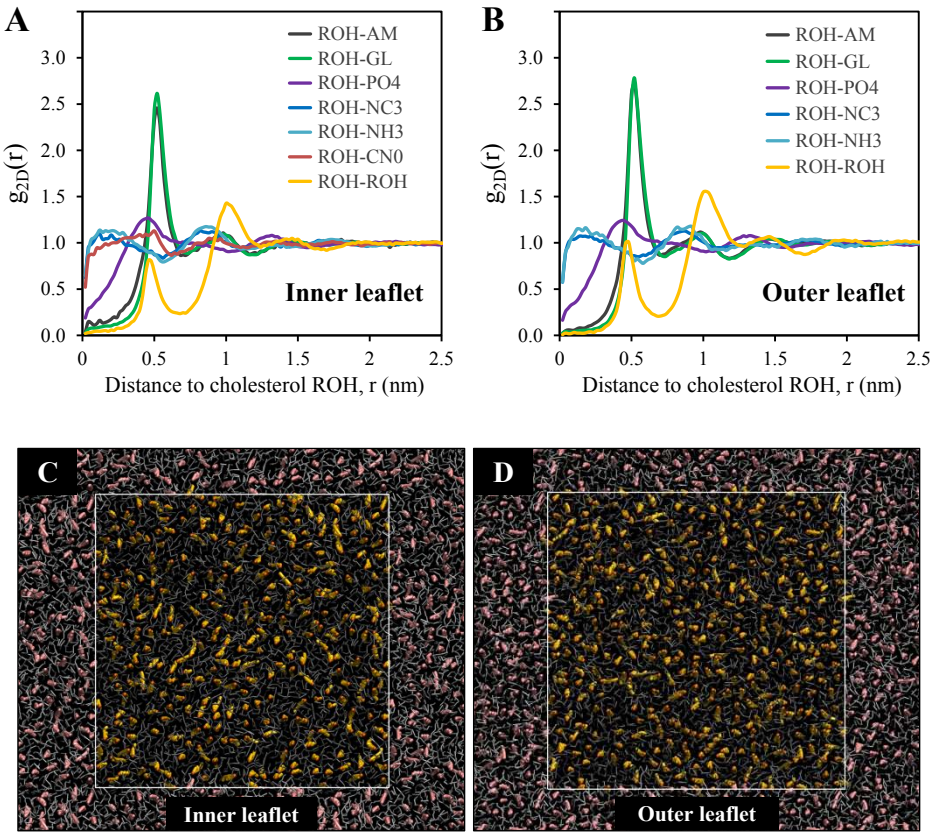

Figure 3. 2D radial distribution function, $g_{2D}(r)$, of different beads of lipids around the hydroxyl headgroup of cholesterol (ROH CG bead) at the **A)** inner leaflet and **B)** outer leaflet of the asymmetric bilayer. ROH headgroup of cholesterol resides in close proximity to the amide (AM) and glycerol (GL) beads of lipids. On the other hand, no significant local structure is observed between ROH and other beads (PO4, phosphate; NC3, choline; NH3, ethanolamine; and CN0, serine). **C)** The top view snapshot of the inner leaflet, and **D)** the bottom view snapshot of the outer leaflet of the asymmetric bilayer after 10 μs long simulation. The white boundary is the boundary of the simulation box with periodic images outside of it. The cholesterol molecules and phospholipids are colored yellow and gray, respectively, within the simulation box, and pink and silver outside the simulation box. The hydroxyl headgroup of cholesterol is shown in orange.

The 2D RDF between cholesterol molecules, the ROH-ROH $g_{2D}(r)$, shows that cholesterol molecules do not cluster together but rather are separated by phospholipids molecules. This observation is in accordance with the "umbrella model" that postulates that cholesterol molecules are hidden from water by the phospholipid head groups. If cholesterol molecules were to cluster together then they would get exposed to water.[51,52] This is also confirmed by **Figure 3C** and **D**, which show the top and bottom view snapshots of the leaflets, respectively. **Figure 4** shows the three-dimensional radial distribution function, g(r) between the water molecules and the headgroup of the phospholipids and cholesterol. This g(r) shows that the headgroups of the phospholipids are solvated by water, whereas those of cholesterol are hidden from water, further confirming the umbrella model.

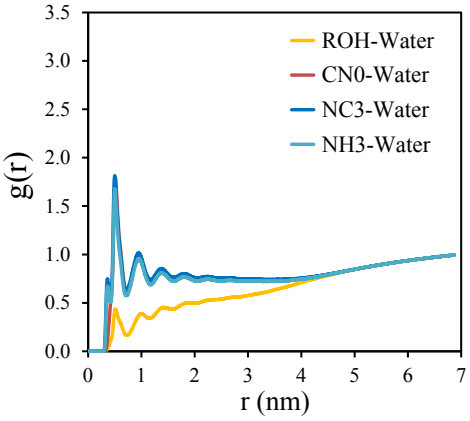

Figure 4. 3D radial distribution function, g(r) of water around the headgroup beads of lipids for the asymmetric system. CN0, NC3, and NH3 represent the headgroup of PS (phosphatidylserine), PC (phosphatidylcholine) & SM (sphingomyelin), and PE (phosphatidylethanolamine) phospholipids, respectively, and ROH represents the hydroxyl headgroup of cholesterol.

3.3. Cholesterol localization as a function of phospholipid structural properties

Our simulations of asymmetric lipid bilayer mimicking those of red blood cells showed that cholesterol distributes unequally between the two leaflets. To investigate the underlying reasons that govern cholesterol distributions in lipid bilayers, we studied various asymmetric bilayers comprising of two kinds of lipids. In these bilayers, one leaflet was always kept as DPPC, while the lipids of the other leaflet were varied. For the sake of convenience of terminology, the DPPC leaflet was labeled as the "outer" leaflet and the other leaflet as the "inner" leaflet. The types of lipids in the inner leaflet were selected so as to isolate the effect of lipids' backbone, headgroup, acyl chain saturation, and acyl chain length on cholesterol distribution. The compositional details of these lipid bilayers are listed in **Table 2**. The snapshot of DPPEi/DPPCo/CHOL lipid bilayer is displayed in **Figure S2**.

Table 2. Composition of asymmetric bilayers with DPPC in the outer leaflet. Cholesterol was present in all the bilayers with a molar ratio of 1:2 with respect to the total number of lipids. The "i" and "o" subscripts represent the inner and outer leaflets, respectively.

Feature	Composition	Headgroup	Backbone	Saturation	Chain length LIPIDi/LIPIDo
Control	DPPCi/DPPCo/CHOL	Choline	glycerol	saturated	16-16/16-16
Backbone	16:0SMi/DPPCo/CHOL	Choline	sphingosine	saturated	16-16/16-16
Headgroup type	DPPEi/DPPCo/CHOL	ethanolamine	glycerol	saturated	16-16/16-16
	DPPSi/DPPCo/CHOL	Serine	glycerol	saturated	16-16/16-16
Acyl chain saturation	DOPCi/DPPCo/CHOL	Choline	glycerol	unsaturated	18-18/16-16
	POPCi/DPPCo/CHOL	choline	glycerol	mono-unsaturated.	16-18/16-16
Acyl chain length	12:0PCi/DPPCo/CHOL	choline	glycerol	saturated	12-12/16-16
	24:0PCi/DPPCo/CHOL	choline	glycerol	saturated	24-24/16-16

As before, all the simulations were performed at 37 °C; the molar ratio of cholesterol to the total number of lipids was kept 1:2; and cholesterol molecules were equally divided between the two leaflets initially. As a control, a symmetric DPPCi/DPPCo/CHOL system was also examined. For this system, as expected, cholesterol was equally distributed between the two leaflets (**Figure 5A**, left panel).

The effect of the lipid backbone. The role of lipid backbone in modulating cholesterol distribution was studied from a system containing cholesterol, 16:0 SM in the inner leaflet, and DPPC in the outer leaflet (16:0SMi/DPPCo/CHOL). The headgroup of SM and DPPC is the same but their backbone is different. SM has polar moieties in the backbone (AM1 and AM2), which are missing in DPPC. It was observed that cholesterol molecules have a higher concentration in the 16:0 SM leaflet compared to the DPPC leaflet (**Figure 5A**, right panel). It is understood that the sphingosine backbone containing the amide groups have a stronger interaction with the headgroup of cholesterol, which agrees well with the experimental studies.[11,12]

The effect of the lipid headgroup. The effect of the lipid headgroup was studied in a lipid bilayer with the outer leaflet as DPPC and the inner leaflet as DPPE or DPPS. It was observed that cholesterol has a stronger affinity for the lipids with serine (DPPS) and ethanolamine (DPPE) headgroups than the lipids with a choline headgroup (DPPC) (**Figure 5B**). This finding is in agreement with the suggestion that PE, which is known to predominantly exist in the inner leaflet of the PM,[5,7,8] draws cholesterol to that leaflet (for complete discussion see[16]).

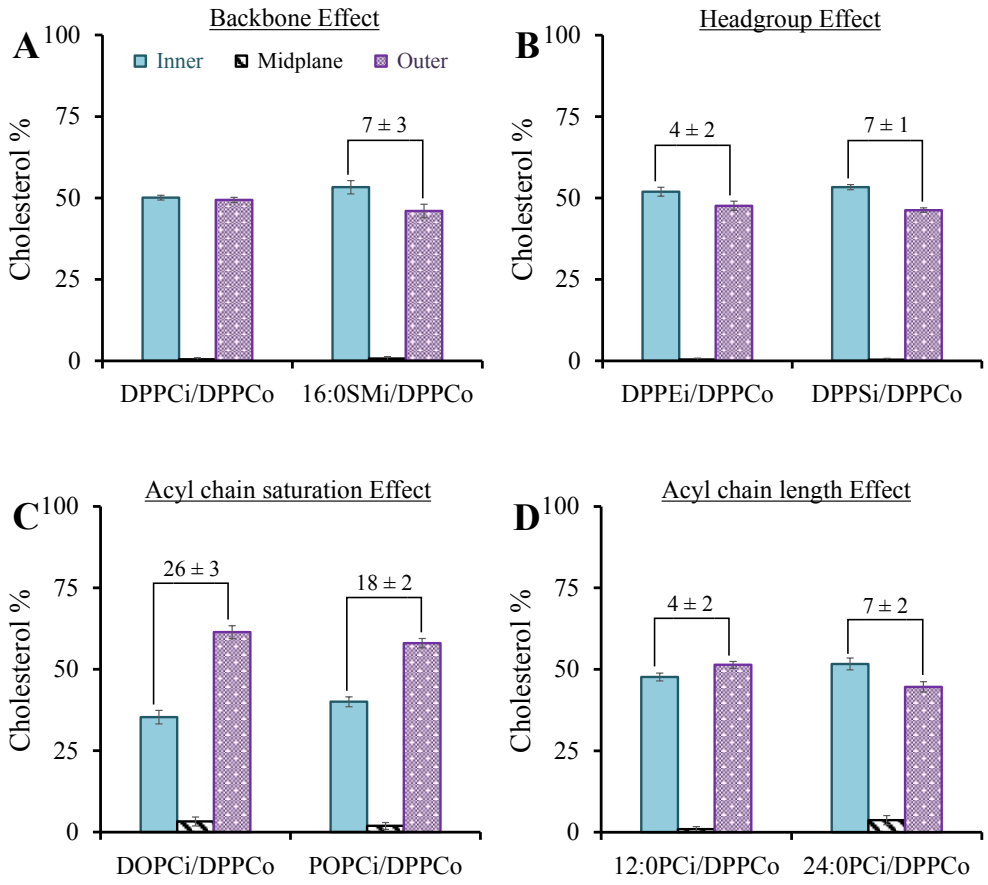

Figure 5. Cholesterol distribution within different asymmetric bilayers (inner leaflet: cyan, midplane: black striped, and the outer leaflet: purple). The effect of lipids' **A)** backbone, **B)** headgroup, **C)** acyl chain saturation and **D)** acyl chain length were analyzed. In all the systems, the outer leaflet was taken as DPPC, and the lipid type of the inner leaflet was varied.

The effect of the acyl chain saturation. Next, the distribution of cholesterol was examined in two bilayers: with DPPC in the outer leaflet, the first bilayer had DOPC (with two unsaturated acyl chains), and the second bilayer had POPC (with one unsaturated acyl chain) in the inner leaflet. In both cases, cholesterol was found to localize in the leaflet with more saturated lipids (**Figure 5C**), in agreement with previous reports.[45,50,53,54] Importantly, the difference in cholesterol distribution between the two leaflets of these systems was much more significant than the other systems studied by us. In accordance with previous studies,[44] we find higher amount of cholesterol in the mid-plane for the DOPCi/DPPCo bilayer as compared to the POPCi/DPPCo bilayer as DOPC has higher degree of unsaturation than POPC. One explanation is that unsaturated lipids with disordered acyl chains do not allow proper alignment of cholesterol in the leaflet.

The effect of the acyl chain length. To examine the role of lipid chain length in cholesterol distribution, bilayers containing DPPC in the outer leaflet and 12:0 PC or 24:0 PC in the inner leaflet were studied (**Figure 5D**). In both cases, cholesterol was preferentially localized in the leaflet that had lipids with longer acyl chain length. A previous study by Courtney et al. reported that cholesterol is enriched in the inner leaflet where shorter lipids are located as compared to the outer leaflet where long chain sphingolipids exist.[17] While in our study, the inner and the outer leaflets have the same headgroup, backbone, and chain saturation, Courtney el al. used a variety of different lipids in the two leaflets, and thus did not isolate the effect of the acyl chain length.

From these studies, it was found that acyl chain saturation results in the strongest asymmetrical distribution followed by the lipid backbone, the headgroup type, and the acyl chain length. Characteristics of these bilayer systems, such as the area per lipid, bilayer thickness, S_{Chain} and cholesterol flip-flop rates are tabulated in **Table S2** (Supporting Information). To understand the relationship between cholesterol distribution and the ordering of lipids in the bilayer, the ratio of the distribution of cholesterol in the inner and the outer leaflets versus the ratio of the S_{Chain} of the lipids in the inner and the outer leaflets was plotted (**Figure 6A**). Interestingly, for all bilayers, the data lies close to the y = x line, implying that the ratio of distribution of cholesterol is similar to the ratio of the ordering of lipids in the leaflets. This striking result suggests that there is a unifying principle governing the distribution of cholesterol in lipid bilayers. It is well understood that cholesterol promotes ordering of lipids in the leaflets. Therefore, it is like a chicken-or-egg conundrum as to whether the ordering of the lipid bilayers governs the observed cholesterol distribution or is it the distribution of cholesterol that results in the ordering of the lipids. To answer this question, we performed simulations of the asymmetric lipid bilayers without any cholesterol to calculate their S_{Chain}. In **Figure 6B** we have plotted the ratio of cholesterol distribution in these bilayers obtained previously with respect to the ratio of the S_{Chain} of the leaflets when cholesterol was absent. A positively sloped linear relationship between the distribution of cholesterol and the ordering in the two leaflets (in the absence of cholesterol) is observed. This result suggests that the distribution of cholesterol is dictated by the relative ordering of the lipids. Certainly, the presence of cholesterol increases the S_{Chain}, but it is not the sole effect underlying the relationship observed in **Figure 6A**. The S_{Chain} of the lipids in both leaflets in the presence and absence of cholesterol is summarized in **Table S3**.

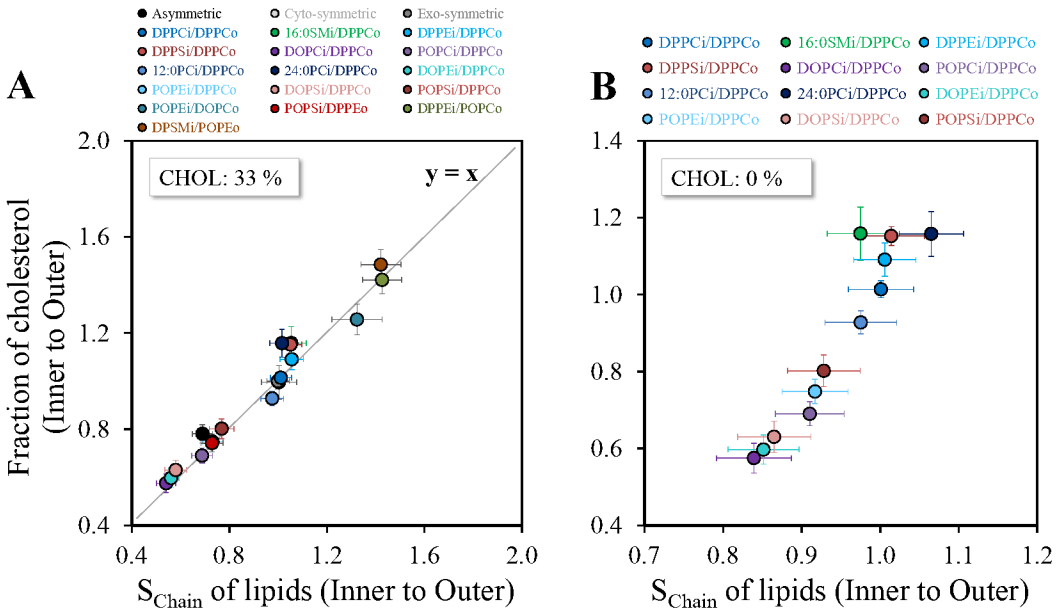

Figure 6. A) Relationship between cholesterol localization in the leaflets with respect to the average order parameter (S_{Chain}) of lipids. The ratio of cholesterol in the inner and outer leaflets lies close to the ratio of S_{Chain} of lipids in the inner and outer leaflets. **B)** Ratio of fraction of cholesterol in the inner and outer leaflets for different lipid bilayers plotted as a function of the ratio of the S_{Chain} of lipids in the same bilayers but in the absence of cholesterol. A positively sloped linear relationship is observed. This figure corresponds to the systems with the same number of two-chain lipids in the inner and outer leaflets.

To explain the distribution of cholesterol observed in the equimolar asymmetric bilayers, we studied symmetric bilayers comprised of the lipid types studied above with a mole fraction of cholesterol equal to 0.33. **Table S4** reports the area per lipid, *a(x)* of these bilayers. It is observed that different bilayers have different *a(x),* which implies that in the equimolar asymmetric bilayers, the leaflet with smaller *a(x)* is under tensile stress and the other one is under compressive stress. Therefore, to relieve these stresses, we constructed "relaxed" asymmetric bilayers by taking the number of lipids + cholesterol in each leaflet as the overall area of the bilayer divided by the *a(x)* of the leaflet (**Table S4**). Therefore, in these asymmetric bilayers, each leaflet now retained its *a(x)* equal to the value found in its symmetric bilayer. For these asymmetric bilayers, we did not find any significant transfer of cholesterols between the leaflets. Interestingly, this implies that cholesterol molecules transfer between the leaflets of equimolar asymmetric bilayers in order to relieve the stresses. Interestingly, we find that the *a(x)* of the leaflets of the equimolar asymmetric bilayers is same as that of symmetric bilayers of these lipids. An interesting question that arises from our results is whether the naturally occurring asymmetric bilayers are equimolar in lipid composition or have different number of lipids in the two leaflets so as to relieve stress. In prior work on synthetic

asymmetric bilayers, the researchers have assumed equimolar lipid composition in the leaflets.[56] In this case, one would expect cholesterol to get re-distributed to relieve the stress.

To estimate the contribution of cholesterol and lipid molecules on the area per lipid of a leaflet, one can calculate the partial molar areas as suggested by Edholm and Nagle.[55] We have performed this calculation on the DPPC/CHOL and DOPC/CHOL symmetric bilayers. The partial molar areas of cholesterol and lipid, $a_{chol}(x)$ and $a_{lipid}(x)$, can then be estimated based on Equations 3 and 4:

$$a_i(\mathrm{x}) = \left(\frac{\partial A(N_1,\ldots,N_m)}{\partial N_i}\right)_{N_{j\neq i}} \qquad \text{Equation 3}$$

$$a_{chol}(\mathrm{x}) = a(x) + (1-x)\frac{\partial a(x)}{\partial x} \quad \text{and} \quad a_{lipid}(\mathrm{x}) = a(x) - x\frac{\partial a(x)}{\partial x} \qquad \text{Equation 4}$$

Figure 7 shows a plot of *a(x)* versus *x* for DPPC/CHOL and DOPC/CHOL symmetric bilayers. It is observed that for the DOPC/CHOL bilayer, the $a_{chol}(x)$ and $a_{DOPC}(x)$ do not vary with *x* and are found to be $a_{chol}(x)$ = 0.21 ± 0.01 nm^2 and $a_{DOPC}(x)$ = 0.69 ± 0.01 nm^2. In the case of DPPC/CHOL bilayer, the partial molar areas depend on *x* and are listed in **Table S5**. In the case of DPPC/CHOL, the $a_{chol}(x)$ is close to zero for small values of cholesterol mole fraction. This result, which has been reported before[55], is due to the condensation effect wherein lipids in the vicinity of cholesterol molecules get more ordered resulting in only a small increase or even a decrease in the area. As the concentration of cholesterols increase, the effect of addition of one more cholesterol molecule is smaller and thus the $a_{chol}(x)$ increases. The S_{chain} of the DOPC/CHOL and DPPC/CHOL bilayers are listed in **Table S5.** It is observed that the S_{chain} in the case of DOPC/CHOL bilayers changes linearly from 0.23±0.02 to only 0.37±0.02 as the cholesterol amount increases from 0% to 50%. Therefore, the condensation effect in this case is weak and the partial molar areas of cholesterol and lipids remain constant as a function of cholesterol concentration. On the other hand, in the case of DPPC/CHOL bilayers, the S_{chain} increases non-linearly and at a more appreciable rate from 0.40±0.02 to 0.79±0.02 indicating that the condensation effect is strong. As a result, the partial molar areas of cholesterol and lipids vary with cholesterol concentration.

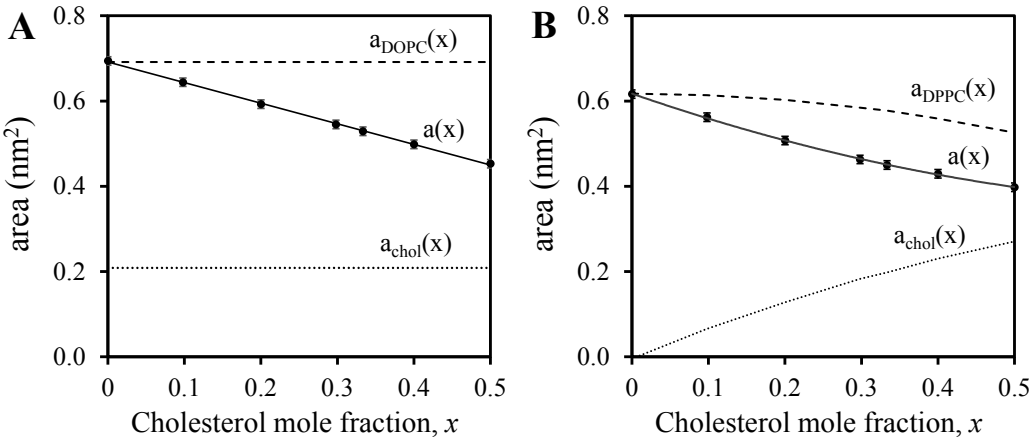

Figure 7. Area per lipid, $a(x)$, as a function of cholesterol mole fraction, $x = N_{chol}/(N_{lipid} + N_{chol})$, for **A)** DOPC/CHOL and **B)** DPPC/CHOL symmetric bilayers. The $a(x)$ for the DOPC/CHOL bilayer varies linearly with x implying that the $a_{DOPC}(x)$ and $a_{chol}(x)$ are constants. On the other hand, the $a(x)$ for the DPPC/CHOL bilayer shows some curvature implying that the partial molar areas are not constants for this bilayer.

4. Conclusions

We have studied the distribution of cholesterol in various asymmetric bilayers. In the bilayer mimicking the composition of the bilayer of red blood cells, we report that cholesterol is enriched in the outer leaflet, which is comprised of more saturated phospholipids, and which shows a higher lipids chain order than the inner leaflet. By studying the distribution of cholesterol in several other equimolar asymmetric bilayers, we show that the distribution of cholesterol is strongly coupled to the ordering of lipids in the leaflets. In fact, our results demonstrate that the ratio of the distribution of cholesterol in the leaflets is close to the ratio of the chain order parameter of lipids in the two leaflets. This observation provides a quantitative relationship for predicting the distribution of cholesterol in equimolar asymmetric lipid bilayers. By simulating the lipid bilayers devoid of any cholesterol, we conclude that the ordering of the lipids in the leaflets governs the distribution of cholesterol in these bilayers. Ordering of lipids in the bilayers dictate the value of area per lipid. Since the area per lipid values for different lipid types is different, equimolar asymmetric bilayers are under mechanical stress: the leaflet with smaller area per lipid, that is higher lipid order, is under tensile stress and the other one (smaller lipid order) is under compressive stress. Therefore, transfer of cholesterol molecules occurs from the leaflet with compressive stress to the one with tensile stress. Interestingly, we find that the area per lipid of the leaflets of asymmetric bilayers remain the same as for the symmetric bilayers. Our findings indicate that in asymmetric lipid bilayers, the distribution of cholesterol is chiefly governed by the tendency to alleviate the mechanical stresses between the two leaflets. Differences in the affinity of cholesterol and various lipid species is not dictating the cholesterol distribution. However, one

would presume that in case there is some strong specific interaction between cholesterol and a lipid type, then such an interaction will also affect the cholesterol distribution. Furthermore, our results show that the cholesterol flip-flop rate is also a function of ordering of lipids in the bilayer. The more ordered lipids are in the leaflets, the lower is the flip-flop rate. Cholesterol is understood to play an important role in modulating the physical and biological characteristics of lipid bilayers. Our findings highlight the strong relationship between cholesterol distribution and lipids ordering within asymmetric lipid bilayers and therefore provides useful insights in the field.

5. Author contributions

Mohammadreza Aghaaminiha: Methodology, Software, Validation, Formal Analysis, Writing – Original Draft, Investigation, Visualization. **Amir Farnoud:** Methodology, Writing – Review & Editing. **Sumit Sharma:** Conceptualization, Methodology, Writing – Review & Editing, Supervision, Project administration, Funding acquisition.

6. Conflict of interest

The authors declare no conflict of interest.

7. Acknowledgments

SS acknowledges the support from National Science Foundation (NSF) grant CDS&E 1953311. The computational resources for this research were provided by the NSF XSEDE grant DMR190005. SS thanks Ohio University Supercomputer Support Fund for covering the computational costs of resources provided by the Ohio Supercomputer Center. We would also like to thank the anonymous reviewer who suggested that we should study asymmetric lipid bilayers with internal stresses removed to identify if internal stresses in asymmetric bilayers are responsible for cholesterol distribution in the leaflets.

8. References

1 G. van Meer, D. R. Voelker and G. W. Feigenson, Membrane lipids: where they are and how they behave, *Nat. Rev. Mol. Cell Biol.*, 2008, **9**, 112–124.

2 H. I. Ingólfsson, T. S. Carpenter, H. Bhatia, P.-T. Bremer, S. J. Marrink and F. C. Lightstone, Computational Lipidomics of the Neuronal Plasma Membrane, *Biophys. J.*, 2017, **113**, 2271–2280.

3 H. I. Ingólfsson, M. N. Melo, F. J. van Eerden, C. Arnarez, C. A. Lopez, T. A. Wassenaar, X. Periole, A. H. de Vries, D. P. Tieleman and S. J. Marrink, Lipid Organization of the Plasma Membrane, *J. Am. Chem. Soc.*, 2014, **136**, 14554–14559.

4 D. Marquardt, B. Geier and G. Pabst, Asymmetric Lipid Membranes: Towards More Realistic Model Systems, *Membranes*, 2015, **5**, 180–196.

5 J. H. Lorent, K. R. Levental, L. Ganesan, G. Rivera-Longsworth, E. Sezgin, M. Doktorova, E. Lyman and I. Levental, Plasma membranes are asymmetric in lipid unsaturation, packing and protein shape, *Nat. Chem. Biol.*, 2020, 1–9.

6 W. Gibson Wood, U. Igbavboa, W. E. Müller and G. P. Eckert, Cholesterol asymmetry in synaptic plasma membranes: Brain membrane cholesterol asymmetry, *J. Neurochem.*, 2011, **116**, 684–689.

7 A. J. Verkleij, R. F. A. Zwaal, B. Roelofsen, P. Comfurius, D. Kastelijn and L. L. M. van Deenen, The asymmetric distribution of phospholipids in the human red cell membrane. A combined study using phospholipases and freeze-etch electron microscopy, *Biochim. Biophys. Acta BBA - Biomembr.*, 1973, **323**, 178–193.

8 A. Vahedi, P. Bigdelou and A. M. Farnoud, Quantitative analysis of red blood cell membrane phospholipids and modulation of cell-macrophage interactions using cyclodextrins, *Sci. Rep.*, 2020, **10**, 15111.

9 J. Liu and J. C. Conboy, 1,2-Diacyl-Phosphatidylcholine Flip-Flop Measured Directly by Sum-Frequency Vibrational Spectroscopy, *Biophys. J.*, 2005, **89**, 2522–2532.

10 D. Marquardt, N. Kučerka, S. R. Wassall, T. A. Harroun and J. Katsaras, Cholesterol's location in lipid bilayers, *Chem. Phys. Lipids*, 2016, **199**, 17–25.

11 B. Ramstedt and J. P. Slotte, Sphingolipids and the formation of sterol-enriched ordered membrane domains, *Biochim. Biophys. Acta BBA - Biomembr.*, 2006, **1758**, 1945–1956.

12 A. Tsamaloukas, H. Szadkowska and H. Heerklotz, Thermodynamic Comparison of the Interactions of Cholesterol with Unsaturated Phospholipid and Sphingomyelins, *Biophys. J.*, 2006, **90**, 4479–4487.

13 P. F. Devaux and R. Morris, Transmembrane Asymmetry and Lateral Domains in Biological Membranes, *Traffic*, 2004, **5**, 241–246.

14 M. Aghaaminiha, S. A. Ghanadian, E. Ahmadi and A. M. Farnoud, A machine learning approach to estimation of phase diagrams for three-component lipid mixtures, *Biochim. Biophys. Acta BBA - Biomembr.*, 2020, **1862**, 183350.

15 W. Wang, L. Yang and H. W. Huang, Evidence of Cholesterol Accumulated in High Curvature Regions: Implication to the Curvature Elastic Energy for Lipid Mixtures, *Biophys. J.*, 2007, **92**, 2819–2830.

16 H. Giang and M. Schick, How Cholesterol Could Be Drawn to the Cytoplasmic Leaf of the Plasma Membrane by Phosphatidylethanolamine, *Biophys. J.*, 2014, **107**, 2337–2344.

17 K. C. Courtney, W. Pezeshkian, R. Raghupathy, C. Zhang, A. Darbyson, J. H. Ipsen, D. A. Ford, H. Khandelia, J. F. Presley and X. Zha, C24 Sphingolipids Govern the Transbilayer Asymmetry of Cholesterol and Lateral Organization of Model and Live-Cell Plasma Membranes, *Cell Rep.*, 2018, **24**, 1037–1049.

18 Y. Lange and J. M. Slayton, Interaction of cholesterol and lysophosphatidylcholine in determining red cell shape., *J. Lipid Res.*, 1982, **23**, 1121–1127.

19 K. John, S. Schreiber, J. Kubelt, A. Herrmann and P. Müller, Transbilayer Movement of Phospholipids at the Main Phase Transition of Lipid Membranes: Implications for Rapid Flip-Flop in Biological Membranes, *Biophys. J.*, 2002, **83**, 3315–3323.

20 K. Leidl, G. Liebisch, D. Richter and G. Schmitz, Mass spectrometric analysis of lipid species of human circulating blood cells, *Biochim. Biophys. Acta BBA - Mol. Cell Biol. Lipids*, 2008, **1781**, 655–664.

21 N. Zehethofer, S. Bermbach, S. Hagner, H. Garn, J. Müller, T. Goldmann, B. Lindner, D. Schwudke and P. König, Lipid Analysis of Airway Epithelial Cells for Studying Respiratory Diseases, *Chromatographia*, 2015, **78**, 403–413.

22 T. L. Steck and Y. Lange, Transverse distribution of plasma membrane bilayer cholesterol: Picking sides, *Traffic*, 2018, **19**, 750–760.

23 S. Garg, L. Porcar, A. C. Woodka, P. D. Butler and U. Perez-Salas, Noninvasive Neutron Scattering Measurements Reveal Slower Cholesterol Transport in Model Lipid Membranes, *Biophys. J.*, 2011, **101**, 370–377.

24 W. F. D. Bennett, J. L. MacCallum, M. J. Hinner, S. J. Marrink and D. P. Tieleman, Molecular View of Cholesterol Flip-Flop and Chemical Potential in Different Membrane Environments, *J. Am. Chem. Soc.*, 2009, **131**, 12714–12720.

25 S. Jo, H. Rui, J. B. Lim, J. B. Klauda and W. Im, Cholesterol Flip-Flop: Insights from Free Energy Simulation Studies, *J. Phys. Chem. B*, 2010, **114**, 13342–13348.

26 T. L. Steck, J. Ye and Y. Lange, Probing red cell membrane cholesterol movement with cyclodextrin., *Biophys. J.*, 2002, **83**, 2118–2125.

27 R. J. Bruckner, S. S. Mansy, A. Ricardo, L. Mahadevan and J. W. Szostak, Flip-Flop-Induced Relaxation of Bending Energy: Implications for Membrane Remodeling, *Biophys. J.*, 2009, **97**, 3113–3122.

28 A. Vahedi and A. M. Farnoud, in *Analysis of Membrane Lipids*, eds. R. Prasad and A. Singh, Springer US, New York, NY, 2020, pp. 143–160.

29 T. L. Steck and Y. Lange, How Slow Is the Transbilayer Diffusion (Flip-Flop) of Cholesterol?, *Biophys. J.*, 2012, **102**, 945–946.

30 S. O. Yesylevskyy, L. V. Schäfer, D. Sengupta and S. J. Marrink, Polarizable Water Model for the Coarse-Grained MARTINI Force Field, *PLOS Comput. Biol.*, 2010, **6**, e1000810.

31 J. Michalowsky, L. V. Schäfer, C. Holm and J. Smiatek, A refined polarizable water model for the coarse-grained MARTINI force field with long-range electrostatic interactions, *J. Chem. Phys.*, 2017, **146**, 054501.

32 S. J. Marrink, H. J. Risselada, S. Yefimov, D. P. Tieleman and A. H. de Vries, The MARTINI Force Field: Coarse Grained Model for Biomolecular Simulations, *J. Phys. Chem. B*, 2007, **111**, 7812–7824.

33 T. A. Wassenaar, H. I. Ingólfsson, R. A. Böckmann, D. P. Tieleman and S. J. Marrink, Computational lipidomics with insane: a versatile tool for generating custom membranes for molecular simulations, *J. Chem. Theory Comput.*, 2015, **11**, 2144–2155.

34 M. J. Abraham, T. Murtola, R. Schulz, S. Páll, J. C. Smith, B. Hess and E. Lindahl, GROMACS: High performance molecular simulations through multi-level parallelism from laptops to supercomputers, *SoftwareX*, 2015, **1–2**, 19–25.

35 G. Bussi, D. Donadio and M. Parrinello, Canonical sampling through velocity-rescaling, *J. Chem. Phys.*, 2007, **126**, 014101.

36 C.-H. Huang, Roles of carbonyl oxygens at the bilayer interface in phospholipid–sterol interaction, *Nature*, 1976, **259**, 242–244.

37 Y. Oh and B. J. Sung, Facilitated and Non-Gaussian Diffusion of Cholesterol in Liquid Ordered Phase Bilayers Depends on the Flip-Flop and Spatial Arrangement of Cholesterol, *J. Phys. Chem. Lett.*, 2018, 6529–6535.

38 S. J. Marrink, A. H. de Vries and A. E. Mark, Coarse Grained Model for Semiquantitative Lipid Simulations, *J. Phys. Chem. B*, 2004, **108**, 750–760.

39 Y. Zhang, A. Lervik, J. Seddon and F. Bresme, A coarse-grained molecular dynamics investigation of the phase behavior of DPPC/cholesterol mixtures, *Chem. Phys. Lipids*, 2015, **185**, 88–98.

40 S. Y. Bhide, Z. Zhang and M. L. Berkowitz, Molecular Dynamics Simulations of SOPS and Sphingomyelin Bilayers Containing Cholesterol, *Biophys. J.*, 2007, **92**, 1284–1295.

41 C. ment Arnarez and J. Uusitalo, Dry Martini, a Coarse-Grained Force Field for Lipid Membrane Simulations with Implicit Solvent, *J. Chem. Theory Comput.*

42 M. R. Krause and S. L. Regen, The Structural Role of Cholesterol in Cell Membranes: From Condensed Bilayers to Lipid Rafts, *Acc. Chem. Res.*, 2014, **47**, 3512–3521.

43 J. Huang, J. T. Buboltz and G. W. Feigenson, Maximum solubility of cholesterol in phosphatidylcholine and phosphatidylethanolamine bilayers, *Biochim. Biophys. Acta BBA - Biomembr.*, 1999, **1417**, 89–100.

44 S. J. Marrink, A. H. de Vries, Thad. A. Harroun, J. Katsaras and S. R. Wassall, Cholesterol Shows Preference for the Interior of Polyunsaturated Lipid Membranes, *J. Am. Chem. Soc.*, 2008, **130**, 10–11.

45 A. B. García-Arribas, A. Alonso and F. M. Goñi, Cholesterol interactions with ceramide and sphingomyelin, *Chem. Phys. Lipids*, 2016, **199**, 26–34.

46 S. Chiantia and E. London, Acyl Chain Length and Saturation Modulate Interleaflet Coupling in Asymmetric Bilayers: Effects on Dynamics and Structural Order, *Biophys. J.*, 2012, **103**, 2311–2319.

47 J. F. Nagle and S. Tristram-Nagle, Structure of lipid bilayers, *Biochim. Biophys. Acta BBA - Rev. Biomembr.*, 2000, **1469**, 159–195.

48 R. Leventis and J. R. Silvius, Use of Cyclodextrins to Monitor Transbilayer Movement and Differential Lipid Affinities of Cholesterol, *Biophys. J.*, 2001, **81**, 2257–2267.

49 J. M. Backer and E. A. Dawidowicz, Transmembrane movement of cholesterol in small unilamellar vesicles detected by cholesterol oxidase., *J. Biol. Chem.*, 1981, **256**, 586–588.

50 N. Kucerka, M.-P. Nieh, J. Pencer, J. N. Sachs and J. Katsaras, What determines the thickness of a biological membrane, *Gen. Physiol. Biophys.*, 2009, **28**, 117–125.

51 H. Martinez-Seara, T. Róg, M. Karttunen, I. Vattulainen and R. Reigada, Cholesterol Induces Specific Spatial and Orientational Order in Cholesterol/Phospholipid Membranes, *PLOS ONE*, 2010, **5**, e11162.

52 J. Dai, M. Alwarawrah and J. Huang, Instability Of Cholesterol Clusters In Lipid Bilayers And The Cholesterol's Umbrella Effect, *J. Phys. Chem. B*, 2010, **114**, 840.

53 S. O. Yesylevskyy and A. P. Demchenko, How cholesterol is distributed between monolayers in asymmetric lipid membranes, *Eur. Biophys. J.*, 2012, **41**, 1043–1054.

54 M. R. Ali, K. H. Cheng and J. Huang, Assess the nature of cholesterol–lipid interactions through the chemical potential of cholesterol in phosphatidylcholine bilayers, *Proc. Natl. Acad. Sci.*, 2007, **104**, 5372–5377.

55 O. Edholm and J. F. Nagle, Areas of Molecules in Membranes Consisting of Mixtures, *Biophys. J.*, 2005, **89**, 1827–1832.

56 Q. Lin and E. London, Preparation of Artificial Plasma Membrane Mimicking Vesicles with Lipid Asymmetry, *PLOS ONE*, 2014, **9**, e87903.